# Excitation cross sections in a collision between two ground-state hydrogen atoms



OPEN ACCESS
IOP Publishing
Journal of Physics B: Atomic, Molecular and Optical Physics
J. Phys. B: At. Mol. Opt. Phys. **54** (2021) 065202 (7pp)
https://doi.org/10.1088/1361-6455/abece3

# Excitation cross sections in a collision between two ground-state hydrogen atoms

**Saed J Al Atawneh**[1,2] **and K Tőkési**[1,*]

[1] Institute for Nuclear Research (ATOMKI), 4026 Debrecen Bem tér 18/c, Hungary
[2] Doctoral School of Physics, Faculty of Science and Technology, University of Debrecen, P.O.400, Debrecen, Hungary

E-mail: tokesi@atomki.hu

Received 8 December 2020, revised 18 February 2021
Accepted for publication 9 March 2021
Published 20 April 2021

**Abstract**

We present excitation cross sections in collision between two ground state hydrogen atoms using a four-body classical trajectory Monte Carlo model. Calculations were performed for impact energies in the range between 1.0 keV and 100 keV where the cross sections are highly relevant to the interest of the fusion research. Beside the total excitation cross sections for target and projectile we also present partial excitation cross sections into the 2s and 2p states of the target. The partial excitation cross sections are compared with the previously obtained theoretical and experimental results.

Keywords: atom–atom collision, excitation, classical trajectory Monte Carlo method

(Some figures may appear in colour only in the online journal)

## 1. Introduction

It is a long history in fusion research to find realistic and precise models and establish a complete databases of cross sections for excitation, ionization, charge transfer, and recombination [1, 2] in the fusion related energy range. Great progress has been made along these lines, but the type of reactions and the collision energy range investigated have been specified mainly by the need to understand the physics of the central core plasma in such magnetically confined plasma devices as tokamaks [1, 3]. The new generation reactors, such as ITER (International thermonuclear experimental reactor) has, however, highlighted the need for new studies of atomic and molecular cross sections. The engineering and also the physics issues are recently focussed on (i) the edge plasma, which must be tailored to suppress the ingress of impurities into the core and to entrain them, and (ii) the divertor, which will be used for hydrogen recycling and heat (power) and particle (impurities, helium ash) exhaust [4, 5]. Because these plasma regimes are characterized by lower temperatures and higher densities than the core, correspondingly different atomic, and even molecular, reactions play crucial roles [5]. We note that in previous years a huge effort was carry out to establish a database for ionization cross sections from intermediate to high collision energies [3, 5]. In order to classify the various theories, it is useful to divide the collisions into three different classes which can be characterized by relative velocity between the projectile ($v$) and the target electron ($v_e$) investigated. These are the followings: (1) the adiabatic energy region ($v \ll v_e$), the intermediate energy region ($v \sim v_e$) and the high-energy region ($v \gg v_e$). In this work we will work in the intermediate and high-energy regions.

Due to the lower temperatures and higher densities, significant amounts of neutrals present in the edge and divertor regions. Since the excitation cross sections for neutral–neutral atoms can be large compared to the ionization channels at low collision energies, these processes may play a dominant role in the momentum balance of these regions [3–5]. In the production of atomic data relevant to fusion energy research a database for excitation and other cross sections related to transport properties has not been compiled so far and even more many processes still lack the cross section data. In particular, the slow, neutral particles are important because of their role

* Author to whom any correspondence should be addressed.

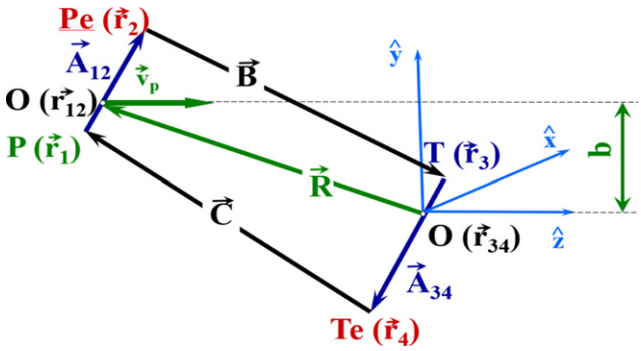


**Figure 1.** The schematic diagram of the four-body collision system. The relative position vectors of the particles involved in four-body collisions. $\vec{A}_{34} = \vec{r}_4 - \vec{r}_3$, $\vec{A}_{12} = \vec{r}_2 - \vec{r}_1$, $\vec{B} = \vec{r}_3 - \vec{r}_2$, $\vec{C} = \vec{r}_1 - \vec{r}_4$, $O(\vec{r}_{12})$, $O(\vec{r}_{34})$ are the position vector of the center-of-mass of the projectile and target systems, and $b$ is the impact parameter.

in radiating and dissipating power and in providing a high-recycling region that shields plasma-facing components from the high heat and particle fluxes [1, 3–5].

Recently, most of the theoretical and experimental work has been performed for $H(1s) + H(1s)$ collisions to study the excitation cross section of $H^*(2s)$ [6, 7], $H^*(2p)$ [7], and electron loss to continuum [8–12]. Flannery [13] applied the four-state impact parameter model with rectilinear trajectories, neglecting electron exchange and translation factors, in a study of $H(1s) + H(1s) \rightarrow H(1s) + H^*(n = 2)$.Later, Bottcher and Flannery [14] included the effects of electron and nuclear exchange in their multi-state impact parameter calculation. We note that the electron translation factors were again neglected. Ritchie [15] performed a two-state impact parameter calculation in which both electron exchange and translation factors were included. The results of previous calculations differ considerably from each other, illustrating the sensitivity of the cross section to the physical assumptions made.

In this work, we present the excitation cross sections in collision between two ground state hydrogen atoms in the range between 1.0 keV and 100 keV. This energy range covers the typical energy conditions of many astrophysical and laboratory plasmas, including the edge plasmas of thermonuclear fusion devices (ITER). Atomic units are used throughout unless stated otherwise.

## 2. Theory

In our model, the four particles (target nucleus, target electron, and projectile electron, and projectile nucleus) are characterized by their masses and charges. Let us denote the projectile nucleus by $P$, the projectile electron by $P_e$, the target nucleus by $T$ and the target electron by $T_e$. The electron–electron interaction is explicitly included in our four-body calculation. At the time ($t = -\infty$) we consider four particles as two separate atoms, consisting of the projectile system ($P$, $P_e$) labeled as particles (1, 2), and the target system ($T$, $T_e$) labeled as particles (3, 4). Initially, both the projectile ($P$, $P_e$) and the target ($T$, $T_e$) are in the ground state. Figure 1 shows the schematic diagram of our present four-body collision system.

In the present CTMC approach, Hamilton's classical equations of motion for the four-body system is solved numerically for a statistically large number of trajectories with initial conditions determined pseudorandomly. The initial electronic state can be obtained from a micro-canonical distribution, with the spherically symmetric orbit satisfying a random Euler's transformation from the two-dimensional Kepler's equation. A micro-canonical ensemble characterizes the initial state of the target and projectile constrained to an initial binding energy of the given shell can be expressed as:

$$\rho_{E_0}(\vec{A}, \dot{\vec{A}}) = K_1 \delta(E_0 - E) = \delta\left(E_0 - \frac{1}{2}\mu_{T,T_e,P,P_e}\dot{\vec{A}}^2 - V(A)\right), \quad (1)$$

where $K_1$ is a normalization constant, $E_0$ is the ionization energy of the active electron, $V(A)$ is the electron and ionic-core potential, $A$ is the length of the vector $\vec{A}$, and $\mu_{T,T_e P,P_e}$ is the reduced mass of particles '$T$', '$T_e$', '$P$', and '$P_e$'. According to the equation (1), the electronic coordinate is confined to the intervals where the equation (2) is verified.

$$\frac{1}{2}\mu_{T_e}\dot{\vec{A}} = E_0 - V(A) > 0, \quad (2)$$

The initial and the final distances $R_i$ and $R_f$ between the projectile and the target are determined by considering that out of the distances the reaction probability is negligibly small. The Hamiltonian of the system can be expressed as:

$$H = \frac{P_p^2}{2m_p} + \frac{P_T^2}{2m_T} + \frac{P_{P_e}^2}{2m_{P_e}} + \frac{P_{T_e}^2}{2m_{T_e}} + \frac{Z_i Z_j}{|r_p - r_T|} - \frac{Z_i Z_j}{|r_p - r_{T_e}|} - \frac{Z_i Z_j}{|r_p - r_{P_e}|} - \frac{Z_i Z_j}{|r_T - r_{T_e}|} - \frac{Z_i Z_j}{|r_t - r_{P_e}|} + \frac{Z_i Z_j}{|r_{P_e} - r_{T_e}|}, \quad (3)$$

where $(r_p, p_p)$,$(r_T, p_T)$, $(r_{P_e}, p_{p_e})$, and $(r_{T_e}, p_{T_e})$ are the positions and momentums of the projectile, the target, the electron on the projectile, and the electron on the target, respectively. From equation (1), the Hamilton's equations are determined by

$$\dot{r}_{ij} = \frac{\partial H}{\partial p}, \qquad \dot{p}_{ij} = -\frac{\partial H}{\partial r}, \quad i = p, t, e_p, e_t; \;\; j = x, y, z. \quad (4)$$

where

$$\dot{p}_{ij} = \sum_{i \neq j} Z_i Z_j \frac{|r_i - r_j|}{|r_i - r_j|^3}, \quad (5)$$

and

$$\dot{r}_{ij} = \frac{p_{ij}}{m_{ij}}. \quad (6)$$

The Runge–Kutta–Gill method is employed to numerically integrate the above 18 coupled equations of motions with an ensemble of about $10^6$ primary trajectories for each energies. A large number of trajectories are usually needed to keep statistical uncertainties less than 1%. The total and state selective cross sections can by calculated by

$$\sigma_p = \frac{N_P}{N}\pi b_{max}^2, \quad (7)$$

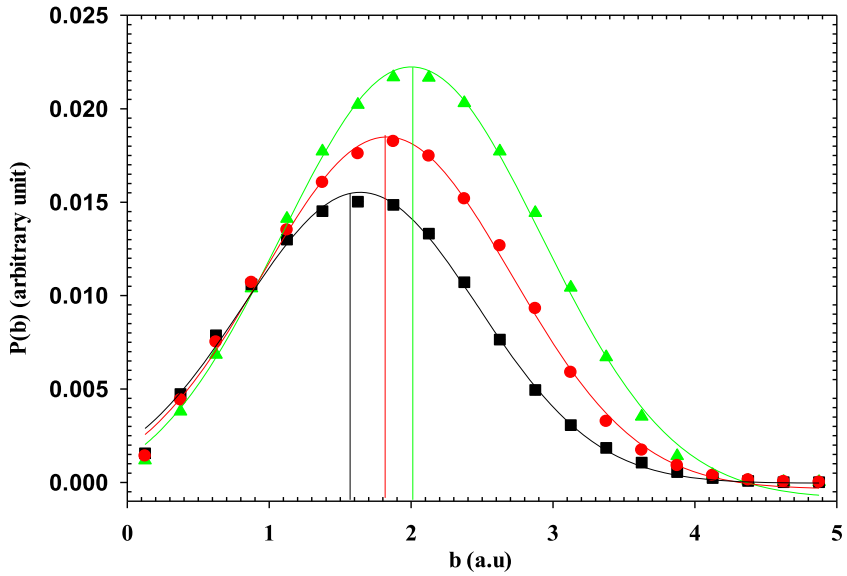


**Figure 2.** Projectile excitation probabilities, when the target atom remains in ground state after the collisions, in collisions between two ground state hydrogen atoms as a function of impact parameter. Black square: the projectile energy is 200 keV. Red circle: the projectile energy is 90 keV. Green triangle: the projectile energy is 20 keV. The lines through the calculated data are the results of the best fit 'Gaussian curve' to guide the eyes.

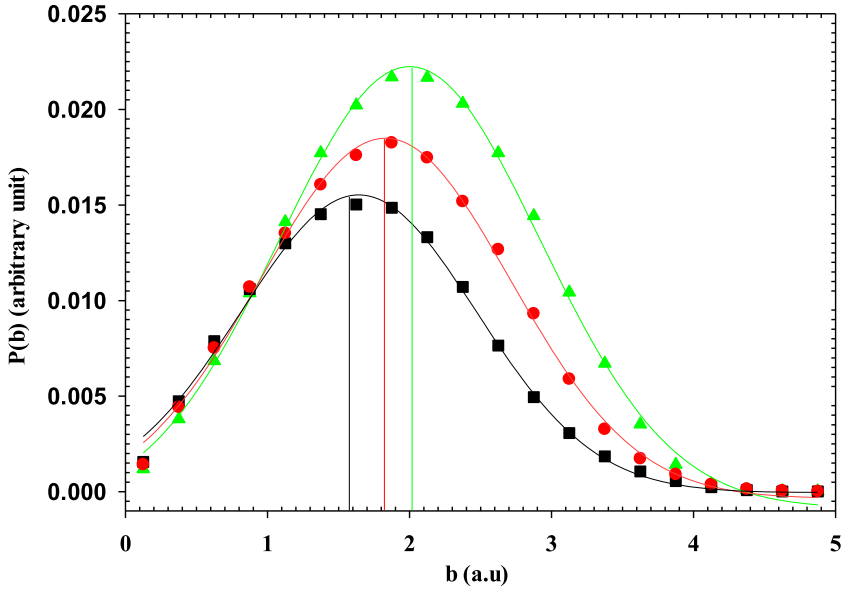


**Figure 3.** Target excitation probabilities, when the projectile atom remains in ground state after the collisions, in collisions between two ground state hydrogen atoms as a function of impact parameter. Black square: the projectile energy is 200 keV. Red circle: the projectile energy is 90 keV. Green triangle: the projectile energy is 20 keV. The lines through the calculated data are the results of the best fit 'Gaussian curve' to guide the eyes.

where $\sigma_p$is the cross section for process P, $N_P$ is the number of trajectories satisfying the criteria for process P with $N$ being the total number of trajectories calculated, and $b_{max}$ is a given largest value of the impact parameter in which the above processes can occur. The statistical uncertainty of the cross section is given by:

$$\Delta\sigma = \sigma_p \left[\frac{N - N_P}{NN_P}\right]^{1/2}. \quad (8)$$

In the CTMC calculations, the energy level $E$ of an electron is determined simply by calculating its binding energy $U = -E$ × A classical principal quantum number is assigned according to

$$n_c = Z_T Z_e \left(\frac{\mu T_e}{2U}\right)^{1/2}. \quad (9)$$

The classical values of $n_c$ are 'quantized' to a specific level $n$ [16] if they satisfy the relation:

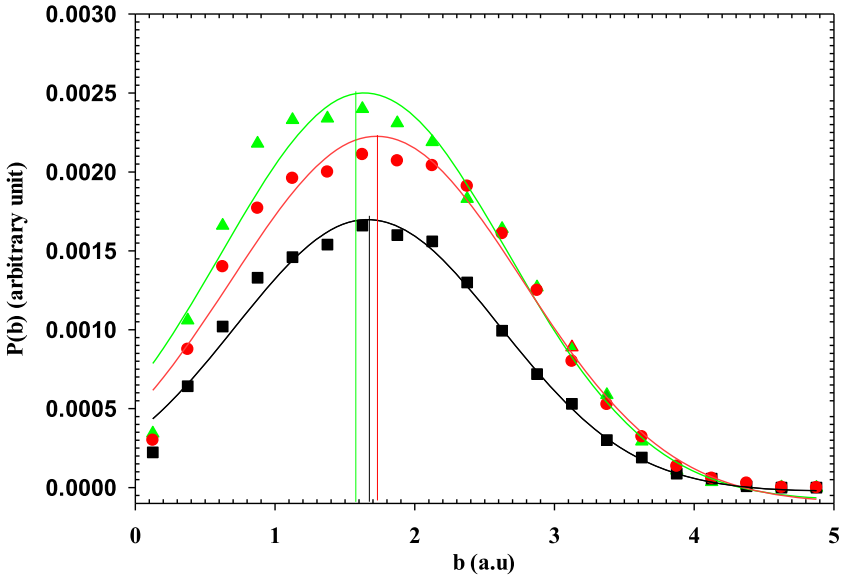


**Figure 4.** Probabilities for the simultaneous excitation of projectile and target in collisions between two ground state hydrogen atoms as a function of impact parameter. Black square: the projectile energy is 200 keV. Red circle: the projectile energy is 90 keV. Green triangle: the projectile energy is 20 keV. The lines through the calculated data are the results of the best fit 'Gaussian curve' to guide the eyes.

$$[(n-1)(n-1/2)n]^{1/3} \leqslant n_c \leqslant [n(n+1/2)(n+1)]^{1/3}. \quad (10)$$

The classical orbital angular momentum is defined by

$$l_c = \sqrt{m_e[(x\dot{y} - y\dot{x})^2 + (x\dot{z} - z\dot{x})^2 + (y\dot{z} - z\dot{y})^2]}, \quad (11)$$

where $x$, $y$, $z$ are the Cartesian coordinates of the electron relative to the nucleus. Since $l_c$ is uniformly distributed for a given $n$ level, the quantal statistical weights are reproduced by choosing bin sizes such that

$$l \leqslant \frac{n}{n_c} l_c \leqslant l + 1, \quad (12)$$

where $l$ is the quantum-mechanical orbital-angular-momentum.

## 3. Result and discussion

To study the collision between two ground state hydrogen atoms, we performed a classical trajectory simulation. In this work, we focus on the investigation of the excitation channels. At first, let us begin with the projectile excitation channel when the target atom remains in ground state after the collisions. This channel can be defined by equation (13) as:

$$H_P\,(1s) + H_T\,(1s) \rightarrow H_P^*\,(n > 1) + H_T(1s), \quad (13)$$

Classically, this channel is a sum of all excitation channels of the projectile. Figure 2 shows the projectile excitation probabilities as a function of impact parameter at 20 keV, 90 keV and 200 keV projectile impact energies respectively. The impact parameter dependent excitation probabilities were fitted by a Gaussian function. The peak maxima of the results of the Gaussian fitting is also shown in figure 2. We found significant difference in the peak maxima of the excitation probabilities. The larger maximum of the impact parameter the lower impact energy. This systematic behaviour can be easy understand with the simple kinematical picture. During the collision the ground state target atom is responsible for the excitation of the projectile. The lower the velocity (energy) of the projectile the more time it spends near the target thereby extending the interaction time. This may indicate that the excitation may have higher probabilities at higher impact parameters. Here we note that the in this case the source of excitation is always the same, namely the ground state target atom.

Our recent collision system is completely symmetric. As a test, we also investigated the total target excitation channel when the projectile remains in ground state after the collisions. This channel can be defined as:

$$H\,(1s) + H\,(Is) \rightarrow H_P\,(1s) + H_T^*\,(n > 1)\,. \quad (14)$$

As for the case of projectile excitation, classically this channel is also a sum of all excitation channels of the target. According to our expectation, we found the same behaviour for the impact parameter dependent excitation probabilities of the target excitation channel when the projectile remained in the ground state after the collision as for the case of projectile excitation with the same conditions (see figure 3). The larger maximum of the impact parameter the lower impact energy.

Last but not the least, we also calculated the total excitation cross sections for the simultaneously excited projectile and target after the collisions. This channel can be described as:

$$H\,(1s) + H\,(Is) \rightarrow H_P^*\,(n > 1) + H_T^*\,(n > 1)\,. \quad (15)$$

This channel is the sum of all excitation cross sections channels of both target and projectile. Figure 4 shows the probabilities for the simultaneous excitation of projectile and target

in collisions between two ground state hydrogen atoms as a function of impact parameter. The impact parameter dependent excitation probabilities show completely different behaviour compared with the previous two cases. We did not recognize a well-defined trend in the peak maxima of the results of the Gaussian fitting. We found that the maximum impact parameters are very close each other as a functions of impact energy. We can say that they are in agreement each other within the estimated uncertainties of our results. This may have in direct consequence of the fact that this channel washes out the results of previous channels and finally we can have an average maximum of the impact parameter resulting the waiting sum of the projectile and target excitation channels.

The corresponding excitation cross sections can be obtained from figures 2–4 by integrated the impact parameter dependent probabilities with respect to the impact parameter. Figure 5 shows the total excitation cross sections as a function of impact energy for projectile excitation when the target remained in its ground state (figure 5(a)), for target excitation when the projectile remained in its ground state (figure 5(b)) and for the simultaneously excited projectile and target in collisions between two ground state hydrogen atoms (figure 5(c)).

Due to the complete symmetry of the collision system, the obtained total excitation cross sections for target and projectile excitations when the partner of the collisions remained in ground state are identical. This channels are the dominant excitation channels. When both collision partner are excited simultaneously the total cross sections are dropped about 10 times smaller and has a maximum around 30 keV. The literature has lack of cross section data for these channels. However, it is available for the partial excitation ones, namely for the target excitation of the 2s and 2p states. Therefore, in the following we present cross section data for these two channels defined as:

$$\mathrm{H_P\,(1s) + H_T\,(1s) \rightarrow H_P\,(1s) + H_T^*(2s),} \qquad (16)$$

$$\mathrm{H_P\,(1s) + H_T\,(1s) \rightarrow H_P\,(1s) + H_T^*(2p).} \qquad (17)$$

Figure 6 shows the excitation cross sections of the target from the 1s state into the 2s state as a function of impact energy. Our results are compared with the calculation of Bottcher and Flannery [14], McLaughlin and Bell [17], Shingal *et al* [18], and with the experimental data of Morgan *et al* [6], and Hill *et al* [19]. Flannery applied the four-state impact parameter model with rectilinear trajectories, neglecting electron exchange, and translation factors. Later, Bottcher and Flannery included the effects of electron and nuclear exchange in their multi-state impact parameter calculation. Ritchie performed a two-state impact parameter calculation in which both electron exchange and translation factors were included. The present CTMC calculations provide a good agreement with the experimental data below 10 keV projectile energy. At the same time, in this energy range, all theories are higher than those of the present CTMC calculations except the

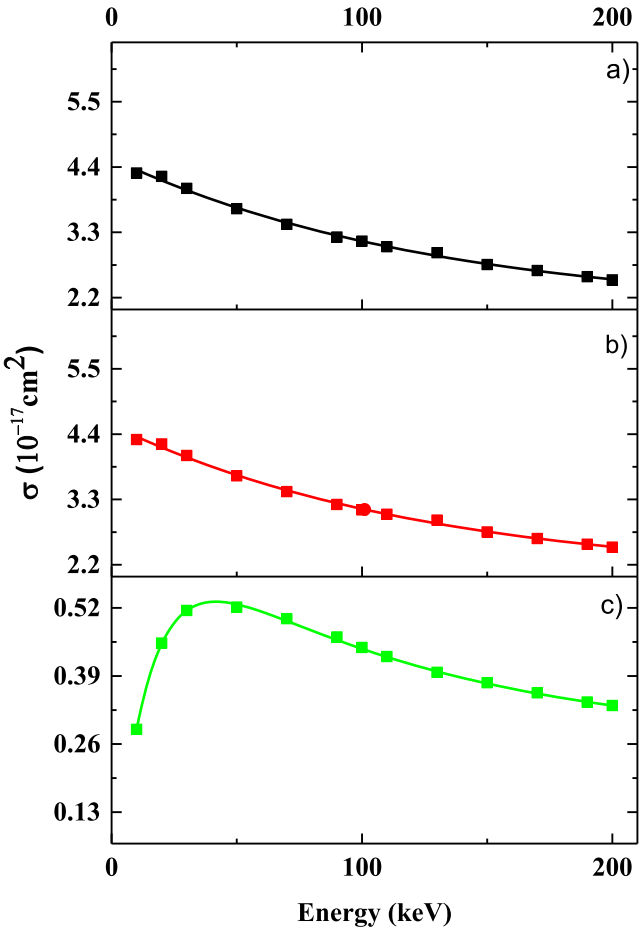


**Figure 5.** The total excitation cross section in a collision between two ground state hydrogen atoms as a function of impact energy. (a) Black square: presents CTMC results for the total projectile excitation cross sections channels defined by equation (13). (b) Red square: presents CTMC results for the total target excitation cross sections channels defined by equation (14). (c) Green square: presents CTMC results for the total simultaneously excited projectile and target sates defined by equation (15). The lines through the calculated data are the results of the best fit to guide the eyes.

Bottcher and Flannery calculation which shows very low cross sections. On the other hand, at high energies, the present CTMC calculations overestimate the experimental and other theoretical observations.

Figure 7 shows our present excitation cross sections of the target from the 1s state into the 2p state as a function of impact energy. Figure 7 also shows the previous results of the 2p target excitation channels by CHEN Lan-Fang *et al* [20], using the CTMC calculation, and by Bottcher and Flannery [14], using the four-state symmetrised exchange calculation. It can be seen that the present CTMC results for 2p target excitation cross sections are close to the previous classical simulation of CHEN Lan-Fang *et al* [20]. Moreover our present results are in good agreement with the experimental data of Morgan *et al* [21]. This good agreement especially valid in the low projectile energy region.

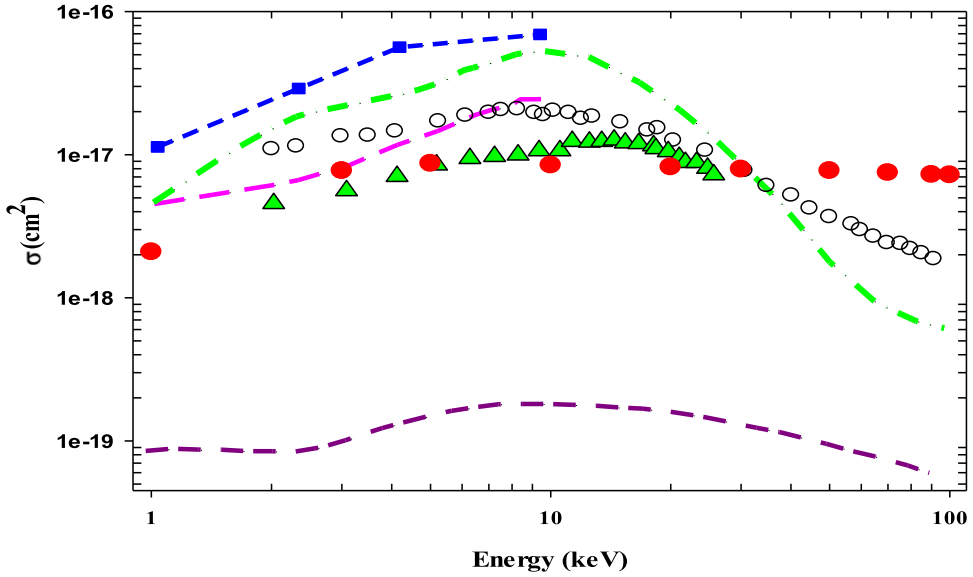


**Figure 6.** Excitation cross sections of the target from 1s state into the 2s state as a function of impact energy in collision between two ground state hydrogen atoms. Red circles: presents CTMC results for 2s target excitation cross sections defined by equation (16). Blue square-dashed line: two-state based calculation by Shingal *et al* [18]. Green dashed-dots: four-state based calculation by Shingal *et al* [18]. Pink dashed line: two-state based calculation by McLaughlin and Bell [17]. Dark pink dashed line: four-state based calculation by Bottcher and Flannery [14]. Open circles: experimental data by Morgan *et al* [6]. Green triangles: experimental data by Hill *et al* [19].

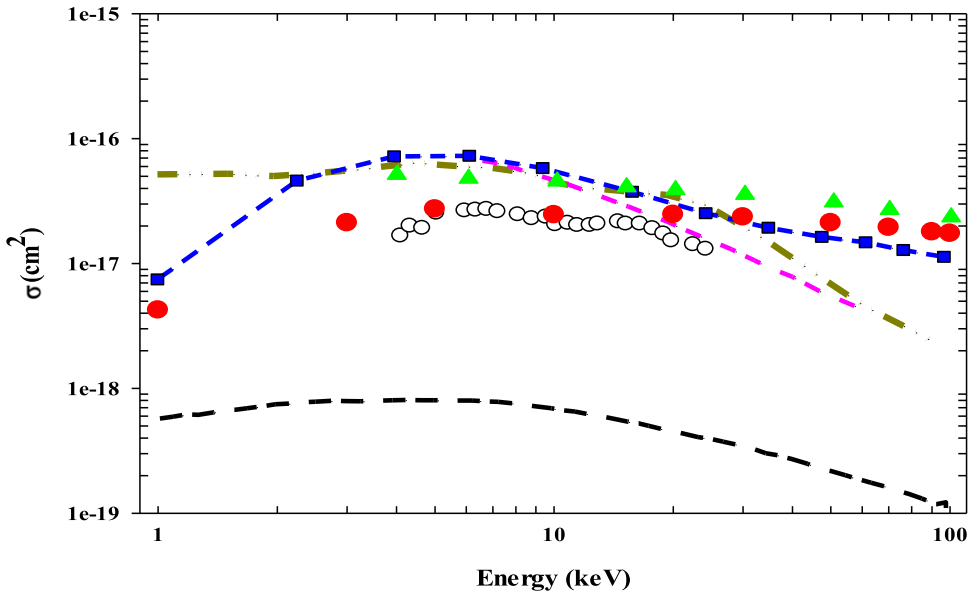


**Figure 7.** Excitation cross sections of the target from the 1s state into the 2p state in collision between two ground state hydrogen atoms as a function of impact energy. Red circles: presents CTMC results for 2p excitation cross sections of the target, defined by equation (17). Green triangles: the CTMC calculation by CHEN Lan-Fang *et al* [20]. Dark yellow dashed-double-dots: four-state results of Shingal *et al* [18]. Pink dashed line: 2p target excitation cross sections calculated by McLaughlin and Bell [22]. Black dashed line: the Four-state results of Bottcher and Flannery [14]. Cross section for $H_P\,(1s) + H_T\,(1s) \rightarrow H_P^*\,(n > 1) + H_T^*(2p)$. Blue square-dashed line: 2p target excitation cross sections calculated by McLaughlin and Bell [22]. Open circles: experimental data by Morgan *et al* [21].

## 4. Conclusion

We presented four-body classical trajectory Monte Carlo simulation of excitation in collisions between two ground state hydrogen atoms. Calculations were performed for impact energies in the range between 1.0 keV and 100 keV where the cross sections are expected relevant to the interest of the fusion research. Beside the total excitation cross sections for target and projectile we also presented partial excitation cross sections into the 2s and 2p states of the target where previous date were available. While we found systematic trend in the impact parameter maximum of the excitation probabilities as a function of impact energy for the target and projectile excitations when the collision partner remained in ground

state after the collision, namely the maximum impact parameter are higher for lower energies, this systematic trend disappear for the channel of simultaneous target and projectile excitation. We also show that the combined target and projectile excitation cross sections are about 10 times smaller than that of the single excitation cross sections of target and projectile. Due to the symmetry of the collisions these latter cross sections are identical. The partial excitation cross sections of the target from the 1s state into the 2s and 2p stats were also calculated. Our recent cross sections for 2s excitation show a good agreement with the experimental data for energy below 10 keV, and show higher values at higher energies. The excitation cross section of 2p shows a good agreement with the experimental data over the energy range between 4 keV and 22 keV.

## Acknowledgment

The work was support by the National Research, Development and Innovation Office (NKFIH) Grant KH126886. This work has been carried out within the framework of the EUROfusion Consortium and has received funding from the Euratom research and training program 2014-2018 and 2019-2020 under Grant Agreement No. 633053. The views and opinions expressed herein do not necessarily reflect those of the European Commission.

## Data availability statement

All data that support the findings of this study are included within the article (and any supplementary files).

## ORCID iDs

Saed J Al Atawneh https://orcid.org/0000-0003-1680-9667
K Tőkési https://orcid.org/0000-0001-8772-8472

## References

[1] Thomas D M, McKee G R, Burrell K H, Levinton F, Foley E L and Fisher R K 2008 *Fusion Sci. Technol.* **53** 487–527
[2] Guszejnov D, Pokol G I, Pusztai I, Refy D, Zoletnik S, Lampert M and Nam Y U 2012 *Rev. Sci. Instrum.* **83** 113501
[3] Schultz D R, Ovchinnikov S Y and Passovets S V 1995 *Atomic and Molecular Processes in Fusion Edge Plasmas* 1st edn ed R K Janev (Berlin: Springer)
[4] Wolfrum E *et al* 2017 *Nucl. Mater. Energy* **12** 18–27
[5] Janev R K, Reiter D and Samm U 2003 *Collision processes in low-temperature hydrogen plasmas (Report No. JUEL–4105)* (Germany) http://hdl.handle.net/10068/260383
[6] Morgan T J, Stone J and Mayo R 1980 *Phys. Rev.* A **22** 1460–6
[7] Hill J, Geddes J and Gilbody H B 1979 *J. Phys. B: At. Mol. Phys.* **12** 2875–82
[8] Hill J, Geddes J and Gilbody H B 1979 *J. Phys. B: At. Mol. Phys.* **12** 3341–8
[9] van Zyl B and Stephen T M 2014 *J. Geophys. Res. Space Physics* **119** 6925–39
[10] McClure G W 1968 *Phys. Rev.* **166** 22–9
[11] Wittkower A B, Levy G and Gilbody H B 1967 *Proc. Phys. Soc.* **91** 862–7
[12] Tőkési K, Wang J and Olson R E 1994 *Nucl. Instrum. Methods Phys. Res.* B **86** 147–50
[13] Flannery M R 1969 *Phys. Rev.* **183** 241–4
[14] Bottcher C and Flannery M R 1970 *J. Phys. B: At. Mol. Phys.* **3** 1600–9
[15] Ritchie B 1971 *Phys. Rev.* A **3** 656–65
[16] Becker R L and MacKellar A D 1984 *J. Phys. B: At. Mol. Phys.* **17** 3923
[17] McLaughlin B M and Bell K L 1989 *J. Phys. B: At. Mol. Opt. Phys.* **22** 763–76
[18] Shingal R, Bransden B H and Flower D R 1987 *J. Phys. B: At. Mol. Phys.* **20** L477–80
[19] Hill J, Geddes J and Gilbody H B 1979 *J. Phys. B: At. Mol. Phys.* **12** L341–4
[20] Lan-Fang C, Xiao-Long Z, Xin-Wen M, Ling L, Bin H, Jian-Guo W and Janev R 2008 *Chin. Phys. Lett.* **25** 2849–52
[21] Morgan T J, Geddes J and Gilbody H B 1974 *J. Phys. B: At. Mol. Phys.* **7** 142–8
[22] McLaughlin B M and Bell K L 1983 *J. Phys. B: At. Mol. Phys.* **16** 3797–804